HHS Public Access

Author manuscript

J Immunol. Author manuscript; available in PMC 2019 November 01.

Published in final edited form as:

J Immunol. 2018 November 01; 201(9): 2824–2831. doi:10.4049/jimmunol.1800839.

EF Hand domain family member D2 is required for T cell cytotoxicity

Michael Peled[*,†], **Matthew A. Dragovich**[*], **Kieran Adam**[*], **Marianne Strazza**[*], **Anna S. Tocheva**[*], **Irving E. Vega**[‡], and **Adam Mor**[*,§,**]

[*]Perlmutter Cancer Center, NYU School of Medicine, New York, NY 10016, USA

[†]Pulmonary Department, The Chaim Sheba Medical Center, Ramat Gan 52620, Israel

[‡]Department of Translational Science and Molecular Medicine, Michigan State University, College of Human Medicine, Grand Rapids, MI 49503, USA

[§]Columbia Center for Translational Immunology, New York, NY 10032

Abstract

Programmed cell death-1 (PD-1) is a major co-inhibitory receptor and a member of the immunological synapse (IS). To uncover proteins that regulate PD-1 recruitment to the IS, we searched for cytoskeleton-related proteins that also interact with PD-1 using affinity purification mass spectrometry. Among these proteins, EF Hand domain family member D2 (EFHD2), a calcium binding adaptor protein, was functionally and mechanistically analyzed for its contribution to PD-1 signaling. EFHD2 was required for PD-1 to inhibit cytokine secretion, proliferation and adhesion of human T cells. Interestingly, EFHD2 was also required for human T cell-mediated cytotoxicity and for mounting an anti-tumor immune response in a syngeneic murine tumor model. Mechanistically, EFHD2 contributed to IS stability, lytic vesicles trafficking, and granzyme B secretion. Altogether, EFHD2 is an important regulator of T cell cytotoxicity, and further studies should evaluate its role in T cell-mediated inflammation.

Introduction

The immunological synapse (IS) is the interface between T cells and antigen presenting cells (APC). The IS consists of segregated clusters of proteins involved in T cell activation. A key member of these clusters is the T cell receptor (TCR) that is engaged by an antigen-loaded major histocompatibility complex on the APC. Productive interactions initiate signaling cascades that result in T cell adhesion, proliferation, and cytokine secretion. When the IS is composed of a cytotoxic T cell and a corresponding target cell (such as a tumor or virally infected cell), lytic granules are released to eliminate the counter cells. To execute these functions, a stable synapse between the T cell and the target cell must be formed. Indeed, TCR-induced synapses are characterized by reorientation of the microtubule-organizing center and substantial actin accumulation at the boundaries of the contact region (1–3).

[**]Correspondence: Adam Mor MD PhD, 630 W 168 St. PH8-406, Columbia University Medical Center, New York NY 10032. Tel (212) 305-0166. am5121@cumc.columbia.edu.

While T cell functions are required for mounting protective immune responses, it can also result in autoimmunity unless tightly regulated. Accordingly, immune responses are restrained by a plethora of mechanisms, including thymic clonal deletion of self-reactive T cells, inhibitory cells such as regulatory T cells, and anti-inflammatory cytokines (i.e., IL-10 and TGF-β). Another important mechanism to restrict immune responses is immune checkpoints. Most of the immune checkpoints are co-inhibitory receptors that directly inhibit signaling downstream of the TCR.

Programmed cell death 1 (PD-1) is a typical co-inhibitory receptor, expressed on activated T cells and clusters in the IS alongside the TCR upon engagement by its ligands, PD-1 ligand 1 (PDL1) or PDL2 (4). PDL1 is widely expressed on both hematopoietic and non-hematopoietic cells, including tumor cells, whereas PDL2 is mainly expressed on APC (5–9). Upon ligation, PD-1 recruits the phosphatase SHP2 to dephosphorylate phosphoproteins downstream of the TCR and to inhibit T cell activation (10–15). PD-1 knockout mice develop inflammatory cardiomyopathy and glomerulonephritis (16, 17), and PD-1 blockade induces potent anti-tumor immune response in patients with various types of malignancies (18, 19).

We have recently utilized affinity purification mass spectrometry (MS) to discover proteins, beside SHP2, that interact with the intracellular tail of PD-1 and regulate its function (14). Since recruitment of PD-1 to the IS is critical for its function (4), we used this data set to screen for proteins that interact with PD-1 and that also regulate IS formation through cytoskeleton organization. Multiple proteins were uncovered, including Swiprosin-1/EF Hand domain family member D2 (EFHD2). EFHD2 knock down (KD) blocked PD-1 inhibitory functions in T cells through inhibition of stable IS formation. However, EFHD2 was also required for T cell-mediated cytotoxicity and for anti-tumor immune response, implying for a pervasive role for this protein in IS formation.

Materials and methods

General reagents

RPMI 1640 medium, Dulbecco's Modified Eagle's Medium (DMEM), Dulbecco's phosphate-buffered saline (DPBS) and fetal bovine serum (FBS) were purchased from Life Technologies. Opti-MEM-I was purchased from Invitrogen. Ficoll-Paque was purchased from GE. Staphylococcus enterotoxin E (SEE) was acquired from Toxin Technology. BCA assay was purchased from Pierce Biotechnology. Poly-L-lysine, puromycin and fibronection were obtained from Sigma.

Cell culture, transfection, and stimulation

Primary human T cells were isolated from whole blood using RosetteSep (Stemcell). Cells were maintained in enriched media at 5% CO_2 at 37°C. Primary murine T cells were isolated from spleens of 10–12 week-old mice, followed by negative selection using Dynabeads (Invitrogen) T cells isolation kit. Jurkat T cells and Raji B cells were obtained from the ATCC and maintained in RPMI medium supplemented with 10% FBS and 100 units/mL penicillin and streptomycin. MC38 cells were provided by Benjamin Neel (NYU)

and maintained in RPMI medium supplemented with 10% FBS and 100 units/mL penicillin and streptomycin. HEK 293T cells were obtained from the ATCC and maintained in 5% CO_2 at 37°C in DMEM media supplemented with 10% FBS and 100 units/mL penicillin and streptomycin. DNA expression constructs were introduced into the cells by nucleofection (Lonza) with efficiency of 50–70%. Cells were stimulated with magnetic beads (ratio of 1:3 cells/beads) conjugated either with anti-CD3 (25%) (UCHT1; R&D) and IgG_1 (75%) (isotype control; Jackson ImmunoResearch), anti-CD3 (25%) and PDL1-Fc (50%) or PDL2-Fc (50%) recombinant proteins (R&D) and IgG_1 (25%), anti-CD3 (25%) and anti-CD28 (25%) (CD28.2; eBioscience) and IgG_1 (50%), or anti-CD3 (25%) and anti-CD28 (25%) and PDL1-Fc (50%). Constructs were introduced into HEK 293T cells using SuperFect transfection reagent (Qiagen) according to the manufacturer's protocol.

Antibodies

Antibodies used for T cell activation were described above. Anti-GFP mAb-agarose (MBL), anti-GFP (Invitrogen), rat anti-mouse CD16/CD32 (Biosciences) and anti-EFHD2 (abcam) antibodies were used as described. Alexa 488 anti-mouse CD3, percp/Cy5.5 anti-mouse CD8a, APC/Cy7 anti-mouse CD45, PE anti-mouse CD4, Alexa 647 anti-mouse FOXP3, PE/Cy7 anti-mouse CD279 (PD-1), BV421 anti-mouse/human CD44, violet 421 IgG_{2b} isotype control, PE/Cy7 IgG_{2b} isotype control and Alexa 647 IgG_{2b} isotype control antibodies were purchased from Biolegend and used as described.

DNA constructs

pMSCV-PD-1-YFP was a generous gift from James Allison (MD Anderson). PD-1-GFP fusion expression constructs were generated through PCR amplification and cloning into pGFP-N1 vector. Residues 192–288 of the PD-1 were used for cloning the tail of PD-1. pEFHD2-Cherry was generated by cloning of the EFHD2 gene from pDONR221-EFHD2 (DNASU) into mCherry-hLC3B-pcDNA3.1 (David Rubinsztein; AddGene # 40827) (20). mCherry-Lifeact-7 was a gift from Michael Davidson (AddGene # 54491). pMD2G and psPAX2 were gifts from Mark Philips (NYU).

Knocking down of *EFHD2*

EFHD2 was stably knocked down in Jurkat T cells by RNA interference using Mission shRNA plasmids (Sigma). Lentiviral particles were generated by transfecting HEK 293T cells with pMD2G, psPAX2, and the shRNA plasmid using SuperFect (Qiagen). T cells were transduced by centrifugation and selected with puromycin. SMARTpool ON-TARGETplus *EFHD2* and non-targeting control siRNA (Dharmacon) were used according to the manufacturer's instruction. For rescue experiments, a 3'-UTR targeting siRNA was used.

Enzyme-linked immunosorbent assay

To determine the concentration of secreted proteins after stimulation, human and mouse IL-2 (Biolegend), human IFN-γ (Biolegend), and mouse Granzyme B (Invitrogen) kits were used according to the manufacturer's protocols. Cells were stimulated as indicated.

Cell proliferation assay

Cell proliferation assay was performed using tetrazolium compound based CellTiter 96 Aqueous One Solution Cell Proliferation (MTS) assay (Promega). T cells were activated with antibodies coated beads and cultured for 4–6 days. MTS cell viability assay performed as indicated, according to the manufacturer's instructions.

Immunoprecipitation, mass spectrometry and western blot analysis

Cell lysates were mixed with anti-GFP monoclonal antibody couple to agarose beads to enrich for GFP tagged proteins according to the manufacturer's protocols (MBL). Pull down lysates were separated by tris-glycine PAGE and transferred to nitrocellulose filters and visualized as previously described (14). Affinity purification MS with GST-tagged PD-1 tail was previously described (14).

Flow cytometry

T cells were stained with fluorescently conjugated antibodies specific for PD-1 in FACS Buffer, washed and fixed in 1% paraformaldehyde. Events were recorded using FACSCalibur (BD), and analyzed using FlowJo software. To obtain single cell suspensions from tumors, tissues were digested and cells were blocked with anti-FcR prior to staining with antibodies against CD3, PD-1, CD44, CD8, CD4, and CD45 (Biolegend). For anti-FOXP3 (Biolegend) staining, cells were fixed and permeabilized using True-Nuclear Transcription Factor Buffer Set (Biolegend). Samples were collected on a LSRII Flow Cytometer (BD), and data were analyzed using FlowJo software.

Static adhesion assay

Static T cell adhesion to fibronectin-coated plates was performed as reported earlier (21).

Conjugate formation assay

SEE (Toxin Technology) loaded Raji B cells (1.5×10^6) were mixed with Jurkat T cells (1.5×10^6), plated on poly-L-lysine (5 μg/ml) coated glass bottom culture 35mm plates (ibidi), and subjected to brief centrifugation prior to imaging. Images were taken with Zeiss 700 confocal microscope and quantified for conjugate formation as previously described (10, 22).

Mice

Animal studies were approved by the New York University institutional animal care and use committee. *EFHD2* knockout mice were generated by by Dr. Irving Vega (Michigan State University). Briefly, disruption of *EFHD2* gene in Embryonic Stem (ES) cells was performed by homologous recombination using a replacement-type targeting vector (Neo-LacZ). ES cells were electroporated with a neomycin (G418)-Lac Z clones. Chimeric males were obtained and breed with C57BL/6 wild-type females for 10 generations. For the syngeneic tumor model, mice were injected on day 0 with 1×10^6 MC38 cells subcutaneously in the right flank. Tumor diameter was measured every 3 days with an electronic caliper and reported as volume using the formula (width^2 × length) × π/6 (23). Mice were sacrificed

when tumors reached the size of 2,000 mm^3. Tumor infiltrating lymphocytes were analyzed as described earlier.

Cytotoxicity assay

Murine splenocytes were cultured with 1 ug/mL SEE and 1000 U/mL mIL-2 (Miltenyi) for 72 hours, followed by isolation of CD8 T cells using isolation kit (Miltenyi). SEE loaded Raji B cells (target cells) were mixed with CD8 T cells at different ratios, as indicated, and cytotoxicity was tested using LDH cytotoxicity kit (ThermoFisher). In some experiments, CD8 T cells were stained with Lysotracker (ThermoFisher) before mixing with Raji cells, plated on poly-L-lysine (5 μg/ml) coated glass bottom culture 35mm plates (ibidi), and subjected to brief centrifugation prior to imaging. Images were taken with Zeiss 700 confocal microscope and analyzed with ImageJ (NIH).

Histopathology

Tumors were fixed in 10% formalin, embedded in paraffin, and cut in 5 μm-thick sections, stained with hematoxylin and eosin or with anti-CD3 (Abcam). Bound antibodies were detected with peroxidase-based staining.

Statistics

Values are reported as means ± SEM. Statistical analyses were performed using Student's *t*-test and ANOVA analysis. All statistical analyses were performed using GraphPad Prism (Ver. 6.0).

Results

Multiple immunological synapse-related proteins interact with the tail of PD-1

To identify proteins that interact with the tail of PD-1 and that are also related to IS formation and stability, we used our previously published data set of the PD-1 interactome (14). As described, GST-tagged PD-1 cytoplasmic tail was utilized to affinity purify interacting proteins that were subsequently identified by MS. 813 proteins that interacted with GST itself were excluded (Fig. 1A). Of the 220 proteins that specifically interacted with PD-1, we considered candidates that were annotated as related to the IS by performing the following query in the GeneCards database (www.genecards.org) (24): "[phenotypes] (immune) AND [all](cytoskeleton synapse)". Accordingly, 19 PD-1 binding proteins were identified (Tab. 1). Pathways analysis (25) confirmed involvement of these proteins in IS-related functions (Fig. 1B), supporting the biological relevance of the identified proteins.

EFHD2 is required for PD-1 inhibitory functions

Among the proteins that interact with PD-1 (Tab. 1), EFHD2 is of particular interest due to the shared autoimmune characteristics of *EFHD2* and *PD-1* deficient mice (26). Co-immunoprecipitation confirmed physical interaction between GFP-PD-1 and endogenous EFHD2 in Jurkat T cells (Fig. 2A). Knocking down *EFHD2* in primary human T cells with inhibitory RNA targeting the 3-UTR of this gene (Sup. 1A) resulted in near complete elimination of the inhibitory effect of PD-1 on IL-2 secretion downstream the antigen

receptor (Fig. 2B). This phenotype was rescued by expressing *EFHD2* lacking the 3-UTR (Fig. 2B). Importantly, PD-1 expression levels were maintained in the absence of *EFHD2* (Sup. 1B). EFHD2 was required for PD-1 inhibitory functions whether PDL1 or PDL2 were used to engage PD-1 (Fig. 2B). EFHD2 was also required for mediating PD-1 inhibitory signals when T cells were stimulated by cross-linking the co-receptor CD28 (Fig. 2C). Knockdown of EFHD2 blocked PD-1 induced ERK dephosphorylation (Sup. 1C). Functionally, EFHD2 was necessary to mediate the inhibitory effects of PD-1 on IFN-γ secretion (Fig. 2D) and adhesion of T cells to fibronectin-coated wells (Fig. 2E). The ability of PD-1 to inhibit IL-2 secretion (Fig. 2F) and proliferation (Fig. 2G) downstream of the TCR were also dependent on EFHD2 in primary mouse T cells isolated from *EFHD2* deficient mice. Altogether, EFHD2 is an essential mediator of PD-1 signaling and functions in both human and murine T cells *in vitro*.

EFHD2 co-localizes with PD-1 in the immunological synapse

To explore whether EFHD2 and PD-1 are localized to the same subcellular compartment in the context of IS formation, we overexpressed Cherry-EFHD2 in Jurkat T cells. EFHD2 protein was distributed to the cytosolic compartment (Fig. 3A; right panel and Sup. 2A), while GFP-PD-1 (Sup. 1D) was localized to the plasma membrane and to a vesicular compartment (Fig. 3A; left panel). When we overexpressed both proteins in the same cell, EFHD2 was partly enriched at the plasma membrane (Fig. 3B; upper panel), but upon activating the cells by PDL1 expressing Raji cells loaded with SEE, both PD-1 and EFHD2 polarized toward the IS (Fig. 3B; lower panel), supporting functional association.

Cytoskeleton organization through actin polymerization is required to establish stable IS and for proper recruitment of key co-receptors (27), including PD-1. A previous study has shown that EFHD2 was localized to areas of actin polymerization (28), and that EFHD2 could promote actin polymerization; hence, we knocked down *EFHD2* in primary human T cells and recorded the localization of GFP-PD-1. As shown, in the absence of *EFHD2*, PD-1 failed to polarize toward the IS (Fig. 3C), indicating that EFHD2 is needed for PD-1 subcellular localization.

To further study the contribution of EFHD2 to synapse formation we cultured primary human T cells deficient of EFHD2 with Raji B cells loaded with SEE and recorded the tightness of the synapses (Sup. 2B). Shortly after co-culturing, 59% of the control cells formed stable conjugates (Fig. 3D), while for the EFHD2 KD cells, only 24% of the cells maintained this phenotype, suggesting that EFHD2 is required to maintain stable IS. During synapse maturation actin is depleted from the center of the synapse (Sup. 2C) (29) and accumulates at the periphery of the contact area between the cells. Actin visualization by fluorescently-tagged Lifeact peptide (30) revealed filamentous actin clearance from the center of the synapse in the control cells, but not in the EFHD2 deficient cells (Fig. 3E). Altogether, these results suggest that EFHD2 is required for the formation and the maturation of the synapse, which affects PD-1 recruitment to the same compartment.

EFHD2 is necessary for anti-tumor immune response in vivo

PD-1 deficient mice demonstrate reduced tumor growth because of increased anti-tumor T cell activity (23). Since EFHD2 is necessary for PD-1 cellular functions and polarization, we anticipated that tumor growth rate in EFHD2 null mice would be reduced. To test that, MC38 murine colon adenocarcinoma cells were implanted subcutaneously in EFHD2 knockout mice, but unexpectedly, tumor growth rates were increased in the null mice compared to the wild type littermates (Fig. 4A and 4B).

Quantification and organization of tumor infiltrating lymphocytes (TIL) failed to explain this unpredicted phenotype in the absence of significant differences between the experimental groups (Fig. 4C and 4D). Flow analysis revealed that both CD4 and CD8 TIL collected from EFHD2 null mice were more activated compared to the control group, as measured by the expression of both PD-1 and the activation marker CD44 (Fig. 4E). Cells isolated from spleens of the same animals did not demonstrate higher percentage of activated T cells (Fig. 4E). There was also no significant difference in the percentage of regulatory T cells among the TIL to explain the increased tumor growth rate in the EFHD2 null mice (Fig. 4F).

EFHD2 is required for T cell induced cytotoxicity

While EFHD2 was necessary for PD-1 signaling and cellular functions (Fig. 2), it was also required for stable IS formation (Fig. 3), a critical constituent for cytotoxic T cell functions. We hypothesized that cytotoxicity in EFHD2 deficient cells is reduced compared to the control cells, explaining the increased tumor growth rate in the former (Fig. 4). To assess that, we used isolated primed CD8 T cells from both WT and EFHD2 null mice and subjected them to super antigen induced cytotoxicity assay (31). EFHD2 was required for effective killing of target cells *in vitro* (Fig. 5A). Even though EFHD2 null lymphocytes were more activated (Fig. 4E), their overall ability to counter tumor cells was limited (Fig. 5A). Mechanistically, polarization of lytic granules towards the synapse in the EFHD2 null T cells was impaired compared with WT cells (Fig. 5B and 5C). In addition, lower levels of the enzyme Granzyme B were released from EFHD2 deficient cells compared to WT control cells (Fig. 5D).

Discussion

PD-1 polarization and trafficking to the IS are necessary for its function as an inhibitory immune checkpoint (4). In order to uncover PD-1 interacting partners that are also required for its localization, we explored our previous data set (14) through GeneCards functional annotation (24). We found that EFHD2, a calcium binding adaptor protein (32–35), physically interacted with PD-1 and also co-localized with it at the IS. EFHD2 was necessary not just for PD-1 trafficking to the IS, but also for PD-1 function *in vitro*. Since *EFHD2* deficient mice show unregulated responses to infectious stimuli and spontaneously develop auto-antibodies (26), and based on our finding that EFHD2 is necessary for PD-1 function *in vitro*, we speculated that *EFHD2* null mice would show resistance to immunogenic tumors (23). However, MC38 tumors exhibited an increased growth rate in the *EFHD2* deficient mice despite an increased expression of cellular activation markers. This unexpected discrepancy is explained, at least in part, by the ability of EFHD2 to control

additional key cellular functions, such as IS formation and cytotoxicity, bedside mediating PD-1 signaling and polarization.

EFHD2 is a 240 amino acids, calcium sensor protein that was originally described in lymphocytes (32). It consists of an N-terminal region of low complexity with an alanine stretch, a functional SH3-binding motif, two functional EF hands and a C-terminal coiled-coiled domain (Sup. 3) (36). The mechanism of the interaction between PD-1 and EFHD2 is unclear. EFHD2 contains SH3-binding motifs, however the tail of PD-1 lacks SH3 and instead contains phosphotyrosine based motifs that can bind to SH2 domains, immunoreceptor tyrosine-based inhibitory motif (ITIM) and the immunoreceptor tyrosine based-switch motif (ITSM) (14). EFHD2 was affinity-purified by both WT PD-1 tail and by the PD-1 Y223F, Y248F tail, which lacks the ITIM and the ITSM (14). Thus, its interaction with PD-1 appears to be tyrosine independent. Remarkably, GRB2 was also found to be a PD-1-binding partner (Tab. 1) (14). GRB2 contains both SH2 and SH3 domains, and thus could potentially link PD-1 and EFHD2. While we and others have shown that the ITIM and ITSM of PD-1 are necessary for SHP2 binding and activation (12, 14), there could be an early and transient interaction between PD-1 and GRB2, which is later taken over by SHP2. Importantly, it was previously demonstrated that the ITIM and ITSM of PD-1 are not required for its clustering (4), implying that an alternative mechanism should be considered

A previous report has already demonstrated that EFHD2 was localized to areas of actin dynamics (28). EFHD2 was localized to the microvilli like protrusions in HMC-1, a mast cell leukemia cell line (37). Moreover, and in agreement with our findings, EFHD2 was recruited to the actin-rich region in Jurkat T cells during T cell activation, and overexpression of EFHD2 enhanced lamellipodia formation and cell spreading, while knock down of this protein resulted in an opposite effect (28). Mechanistically, it was shown that EFHD2 induced actin bundling in the presence of calcium. Our findings also support a role for EFHD2 in actin dynamics, demonstrated by the reduction in the number of stable synapses in the EFHD2 deficient cells and by reduced actin recruitment to the periphery of the synapses. The lack of PD-1 trafficking to the IS, and the reduced polarization of cytotoxic granules, are likely direct consequences of altered actin dynamics secondary to EFHD2 depletion.

The role of EFHD2 in innate and adaptive immune responses was previously studied. However, it was not clear what was the net effect of EFHD2 in different immune cells, in terms of activation or suppression of their function. Kwon et al., reported that EFHD2 enhanced SDF-1-mediated T cell spreading (28), and Kroczek et al., showed that murine EFHD2 was a positive regulator of Syk activity in response to B cell receptor (BCR) stimulation in the murine cell line WEHI231(38). While these studies imply for a pro-inflammatory role for EFHD2, it was also found to block the expression of the anti-apoptotic NF-κB target gene *BCL-XL* (39). It has been proposed that EFHD2 binds calcium directly (33) and therefore participates in a negative feedback loop, preventing NF-κB signaling as a result of BCR activation (36). Others have shown opposing results, where EFHD2 augmented up-regulation of NF-κB target genes in PMA / ionomycin stimulated HMC-1 cells (40). Additional discrepancy is demonstrated by experimental data using the EFHD2 null mice. These mice elicit enhanced Th2 cell-mediated IgE and IgM production as well as

enhanced germinal center formation in response to infection with the helminth Nippostrongylus brasiliensis as compared to WT mice, suggesting that EFHD2 acts as a negative regulator of type 2 immunity (26). However, LPS-induced sepsis resulted in higher mortality, severe organ dysfunction, restrained macrophage recruitment in affected organs, and attenuated inflammatory cytokine production in EFHD2 null mice compared to the WT littermates, implying for a proinflammatory role of EFHD2. This was attributed to impaired bactericidal capacity and decreased HLA-DR expression in EFHD2 null macrophages, secondary to EFHD2 regulation of IFN-γ receptors (41). Thus, EFHD2 pleotropic effect in the innate and adaptive immune response requires further study.

To summarize, our findings show that EFHD2 is necessary for both anti-inflammatory and pro-inflammatory functions of T cells. This is due to its generalized role in regulating both PD-1 signaling and trafficking but also in mediating adhesion, cytotoxic granules polarization and T cell mediated cytotoxicity. The net effect *in vivo*, at least in the MC38 tumor model, points towards a pro-inflammatory role for EFHD2, as tumor growth rate in EFHD2 deficient mice was enhanced, supporting data from the LPS-induced sepsis experiments (41). It is important to note that both the MC38 model and the LPS-induced sepsis model are Th1 directed models (unlike the helminth infection model, which is a Th2 immune response). Thus, EFHD2 may have different functions depending on the stimulus and the course of the immune response, and targeting EFHD2 in Th1-driven autoimmune disorders may have therapeutic benefit.

Supplementary Material

Refer to Web version on PubMed Central for supplementary material.

Acknowledgments

This work was supported by a grant from the NIH (R01 AI25640).

References

1. Stinchcombe JC, Salio M, Cerundolo V, Pende D, Arico M, and Griffiths GM. 2011 Centriole polarisation to the immunological synapse directs secretion from cytolytic cells of both the innate and adaptive immune systems. BMC biology 9: 45. [PubMed: 21711522]
2. Ueda H, Morphew MK, McIntosh JR, and Davis MM. 2011 CD4+ T-cell synapses involve multiple distinct stages. Proceedings of the National Academy of Sciences of the United States of America 108: 17099–17104. [PubMed: 21949383]
3. Das R, Bassiri H, Guan P, Wiener S, Banerjee PP, Zhong MC, Veillette A, Orange JS, and Nichols KE. 2013 The adaptor molecule SAP plays essential roles during invariant NKT cell cytotoxicity and lytic synapse formation. Blood 121: 3386–3395. [PubMed: 23430111]
4. Yokosuka T, Takamatsu M, Kobayashi-Imanishi W, Hashimoto-Tane A, Azuma M, and Saito T. 2012 Programmed cell death 1 forms negative costimulatory microclusters that directly inhibit T cell receptor signaling by recruiting phosphatase SHP2. The Journal of experimental medicine 209: 1201–1217. [PubMed: 22641383]
5. Dong H, Zhu G, Tamada K, and Chen L. 1999 B7-H1, a third member of the B7 family, co-stimulates T-cell proliferation and interleukin-10 secretion. Nature medicine 5: 1365–1369.
6. Freeman GJ, Long AJ, Iwai Y, Bourque K, Chernova T, Nishimura H, Fitz LJ, Malenkovich N, Okazaki T, Byrne MC, Horton HF, Fouser L, Carter L, Ling V, Bowman MR, Carreno BM, Collins M, Wood CR, and Honjo T. 2000 Engagement of the PD-1 immunoinhibitory receptor by a novel

B7 family member leads to negative regulation of lymphocyte activation. The Journal of experimental medicine 192: 1027–1034. [PubMed: 11015443]

7. Latchman Y, Wood CR, Chernova T, Chaudhary D, Borde M, Chernova I, Iwai Y, Long AJ, Brown JA, Nunes R, Greenfield EA, Bourque K, Boussiotis VA, Carter LL, Carreno BM, Malenkovich N, Nishimura H, Okazaki T, Honjo T, Sharpe AH, and Freeman GJ. 2001 PD-L2 is a second ligand for PD-1 and inhibits T cell activation. Nature immunology 2: 261–268. [PubMed: 11224527]
8. Tseng SY, Otsuji M, Gorski K, Huang X, Slansky JE, Pai SI, Shalabi A, Shin T, Pardoll DM, and Tsuchiya H. 2001 B7-DC, a new dendritic cell molecule with potent costimulatory properties for T cells. The Journal of experimental medicine 193: 839–846. [PubMed: 11283156]
9. Juneja VR, McGuire KA, Manguso RT, LaFleur MW, Collins N, Haining WN, Freeman GJ, and Sharpe AH. 2017 PD-L1 on tumor cells is sufficient for immune evasion in immunogenic tumors and inhibits CD8 T cell cytotoxicity. The Journal of experimental medicine 214: 895–904. [PubMed: 28302645]
10. Azoulay-Alfaguter I, Strazza M, Pedoeem A, and Mor A. 2015 The coreceptor programmed death 1 inhibits T-cell adhesion by regulating Rap1. The Journal of allergy and clinical immunology 135: 564–567. [PubMed: 25240786]
11. Chemnitz JM, Parry RV, Nichols KE, June CH, and Riley JL. 2004 SHP-1 and SHP-2 associate with immunoreceptor tyrosine-based switch motif of programmed death 1 upon primary human T cell stimulation, but only receptor ligation prevents T cell activation. Journal of immunology 173: 945–954.
12. Hui E, Cheung J, Zhu J, Su X, Taylor MJ, Wallweber HA, Sasmal DK, Huang J, Kim JM, Mellman I, and Vale RD. 2017 T cell costimulatory receptor CD28 is a primary target for PD-1-mediated inhibition. Science 355: 1428–1433. [PubMed: 28280247]
13. Patsoukis N, Brown J, Petkova V, Liu F, Li L, and Boussiotis VA. 2012 Selective effects of PD-1 on Akt and Ras pathways regulate molecular components of the cell cycle and inhibit T cell proliferation. Science signaling 5: ra46. [PubMed: 22740686]
14. Peled M, Tocheva AS, Sandigursky S, Nayak S, Philips EA, Nichols KE, Strazza M, Azoulay-Alfaguter I, Askenazi M, Neel BG, Pelzek AJ, Ueberheide B, and Mor A. 2018 Affinity purification mass spectrometry analysis of PD-1 uncovers SAP as a new checkpoint inhibitor. Proceedings of the National Academy of Sciences of the United States of America 115: E468–E477. [PubMed: 29282323]
15. Sheppard KA, Fitz LJ, Lee JM, Benander C, George JA, Wooters J, Qiu Y, Jussif JM, Carter LL, Wood CR, and Chaudhary D. 2004 PD-1 inhibits T-cell receptor induced phosphorylation of the ZAP70/CD3zeta signalosome and downstream signaling to PKCtheta. FEBS letters 574: 37–41. [PubMed: 15358536]
16. Nishimura H, Nose M, Hiai H, Minato N, and Honjo T. 1999 Development of lupus-like autoimmune diseases by disruption of the PD-1 gene encoding an ITIM motif-carrying immunoreceptor. Immunity 11: 141–151. [PubMed: 10485649]
17. Nishimura H, Okazaki T, Tanaka Y, Nakatani K, Hara M, Matsumori A, Sasayama S, Mizoguchi A, Hiai H, Minato N, and Honjo T. 2001 Autoimmune dilated cardiomyopathy in PD-1 receptor-deficient mice. Science 291: 319–322. [PubMed: 11209085]
18. Couzin-Frankel J 2013 Breakthrough of the year 2013. Cancer immunotherapy. Science 342: 1432–1433. [PubMed: 24357284]
19. Tumeh PC, Harview CL, Yearley JH, Shintaku IP, Taylor EJ, Robert L, Chmielowski B, Spasic M, Henry G, Ciobanu V, West AN, Carmona M, Kivork C, Seja E, Cherry G, Gutierrez AJ, Grogan TR, Mateus C, Tomasic G, Glaspy JA, Emerson RO, Robins H, Pierce RH, Elashoff DA, Robert C, and Ribas A. 2014 PD-1 blockade induces responses by inhibiting adaptive immune resistance. Nature 515: 568–571. [PubMed: 25428505]
20. Jahreiss L, Menzies FM, and Rubinsztein DC. 2008 The itinerary of autophagosomes: from peripheral formation to kiss-and-run fusion with lysosomes. Traffic 9: 574–587. [PubMed: 18182013]
21. Strazza M, Azoulay-Alfaguter I, Pedoeem A, and Mor A. 2014 Static adhesion assay for the study of integrin activation in T lymphocytes. Journal of visualized experiments : JoVE.

22. Strazza M, Azoulay-Alfaguter I, Dun B, Baquero-Buitrago J, and Mor A. 2015 CD28 inhibits T cell adhesion by recruiting CAPRI to the plasma membrane. Journal of immunology 194: 2871–2877.

23. Woo SR, Turnis ME, Goldberg MV, Bankoti J, Selby M, Nirschl CJ, Bettini ML, Gravano DM, Vogel P, Liu CL, Tangsombatvisit S, Grosso JF, Netto G, Smeltzer MP, Chaux A, Utz PJ, Workman CJ, Pardoll DM, Korman AJ, Drake CG, and Vignali DA. 2012 Immune inhibitory molecules LAG-3 and PD-1 synergistically regulate T-cell function to promote tumoral immune escape. Cancer research 72: 917–927. [PubMed: 22186141]

24. Safran M, Chalifa-Caspi V, Shmueli O, Olender T, Lapidot M, Rosen N, Shmoish M, Peter Y, Glusman G, Feldmesser E, Adato A, Peter I, Khen M, Atarot T, Groner Y, and Lancet D. 2003 Human Gene-Centric Databases at the Weizmann Institute of Science: GeneCards, UDB, CroW 21 and HORDE. Nucleic acids research 31: 142–146. [PubMed: 12519968]

25. Chen J, Bardes EE, Aronow BJ, and Jegga AG. 2009 ToppGene Suite for gene list enrichment analysis and candidate gene prioritization. Nucleic acids research 37: W305–311. [PubMed: 19465376]

26. Brachs S, Turqueti-Neves A, Stein M, Reimer D, Brachvogel B, Bosl M, Winkler T, Voehringer D, Jack HM, and Mielenz D. 2014 Swiprosin-1/EFhd2 limits germinal center responses and humoral type 2 immunity. European journal of immunology 44: 3206–3219. [PubMed: 25092375]

27. Kumari S, Curado S, Mayya V, and Dustin ML. 2014 T cell antigen receptor activation and actin cytoskeleton remodeling. Biochimica et biophysica acta 1838: 546–556. [PubMed: 23680625]

28. Kwon MS, Park KR, Kim YD, Na BR, Kim HR, Choi HJ, Piragyte I, Jeon H, Chung KH, Song WK, Eom SH, and Jun CD. 2013 Swiprosin-1 is a novel actin bundling protein that regulates cell spreading and migration. PloS one 8: e71626. [PubMed: 23977092]

29. Ritter AT, Asano Y, Stinchcombe JC, Dieckmann NM, Chen BC, Gawden-Bone C, van Engelenburg S, Legant W, Gao L, Davidson MW, Betzig E, Lippincott-Schwartz J, and Griffiths GM. 2015 Actin depletion initiates events leading to granule secretion at the immunological synapse. Immunity 42: 864–876. [PubMed: 25992860]

30. Riedl J, Crevenna AH, Kessenbrock K, Yu JH, Neukirchen D, Bista M, Bradke F, Jenne D, Holak TA, Werb Z, Sixt M, and Wedlich-Soldner R. 2008 Lifeact: a versatile marker to visualize F-actin. Nature methods 5: 605–607. [PubMed: 18536722]

31. Rosendahl A, Kristensson K, Riesbeck K, and Dohlsten M. 2000 T-cell cytotoxicity assays for studying the functional interaction between the superantigen staphylococcal enterotoxin A and T-cell receptors. Methods in molecular biology 145: 241–257. [PubMed: 10820726]

32. Vuadens F, Rufer N, Kress A, Corthesy P, Schneider P, and Tissot JD. 2004 Identification of swiprosin 1 in human lymphocytes. Proteomics 4: 2216–2220. [PubMed: 15274114]

33. Vega IE, Traverso EE, Ferrer-Acosta Y, Matos E, Colon M, Gonzalez J, Dickson D, Hutton M, Lewis J, and Yen SH. 2008 A novel calcium-binding protein is associated with tau proteins in tauopathy. Journal of neurochemistry 106: 96–106. [PubMed: 18346207]

34. Hagen S, Brachs S, Kroczek C, Furnrohr BG, Lang C, and Mielenz D. 2012 The B cell receptor-induced calcium flux involves a calcium mediated positive feedback loop. Cell calcium 51: 411–417. [PubMed: 22317918]

35. Vazquez-Rosa E, Rodriguez-Cruz EN, Serrano S, Rodriguez-Laureano L, and Vega IE. 2014 Cdk5 phosphorylation of EFhd2 at S74 affects its calcium binding activity. Protein science : a publication of the Protein Society 23: 1197–1207. [PubMed: 24917152]

36. Dutting S, Brachs S, and Mielenz D. 2011 Fraternal twins: Swiprosin-1/EFhd2 and Swiprosin-2/EFhd1, two homologous EF-hand containing calcium binding adaptor proteins with distinct functions. Cell communication and signaling : CCS 9: 2. [PubMed: 21244694]

37. Ramesh TP, Kim YD, Kwon MS, Jun CD, and Kim SW. 2009 Swiprosin-1 Regulates Cytokine Expression of Human Mast Cell Line HMC-1 through Actin Remodeling. Immune network 9: 274–284. [PubMed: 20157615]

38. Kroczek C, Lang C, Brachs S, Grohmann M, Dutting S, Schweizer A, Nitschke L, Feller SM, Jack HM, and Mielenz D. 2010 Swiprosin-1/EFhd2 controls B cell receptor signaling through the assembly of the B cell receptor, Syk, and phospholipase C gamma2 in membrane rafts. Journal of immunology 184: 3665–3676.

39. Avramidou A, Kroczek C, Lang C, Schuh W, Jack HM, and Mielenz D. 2007 The novel adaptor protein Swiprosin-1 enhances BCR signals and contributes to BCR-induced apoptosis. Cell death and differentiation 14: 1936–1947. [PubMed: 17673920]

40. Thylur RP, Kim YD, Kwon MS, Oh HM, Kwon HK, Kim SH, Im SH, Chun JS, Park ZY, and Jun CD. 2009 Swiprosin-1 is expressed in mast cells and up-regulated through the protein kinase C beta I/eta pathway. Journal of cellular biochemistry 108: 705–715. [PubMed: 19693767]

41. Zhang S, Tu Y, Sun YM, Li Y, Wang RM, Cao Y, Li L, Zhang LC, and Wang ZB. 2018 Swiprosin-1 deficiency impairs macrophage immune response of septic mice. JCI insight 3.

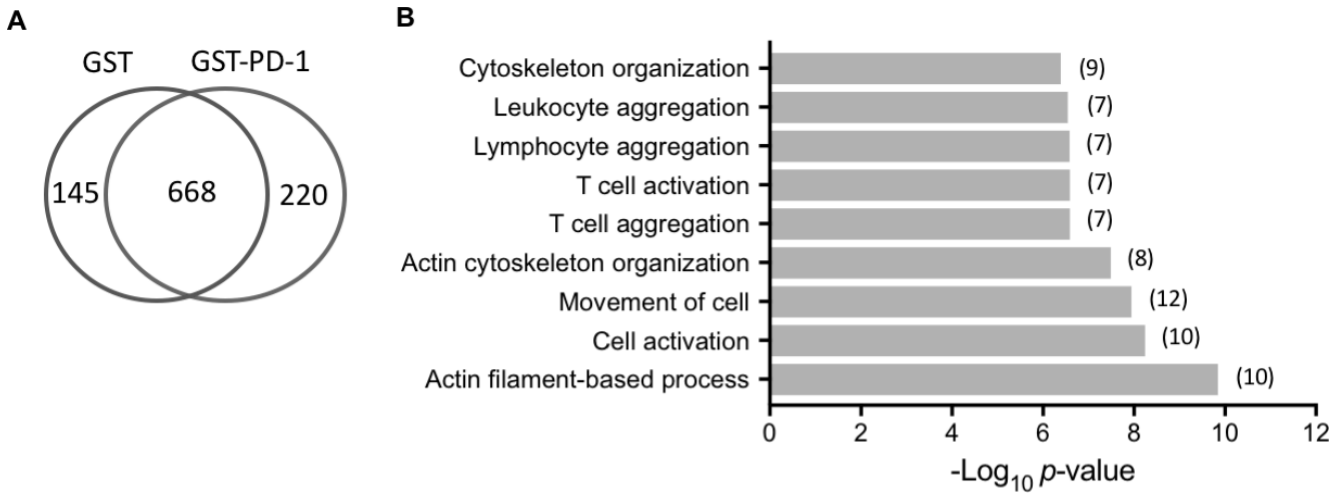

Figure 1. Multiple immunological synapse-related proteins interact with the tail of PD-1.

(A) Venn diagram showing the numbers of proteins that interact with GST or with GST-PD-1. **(B)** Functional pathways enrichment analysis of the proteins that interact specifically with GST-PD-1 and are related to the IS. The top nine significantly enriched functional clusters (Y-axis) are displayed over the corresponding -Log_{10}*p*-value (X-axis). The *p*-value represents the probability of discovering at least x number of genes (x = number in brackets) out of the total number of the genes in the list (n=19, Table 1) annotated to a particular functional cluster given the proportion of genes in the whole genome that are annotated to that functional cluster.

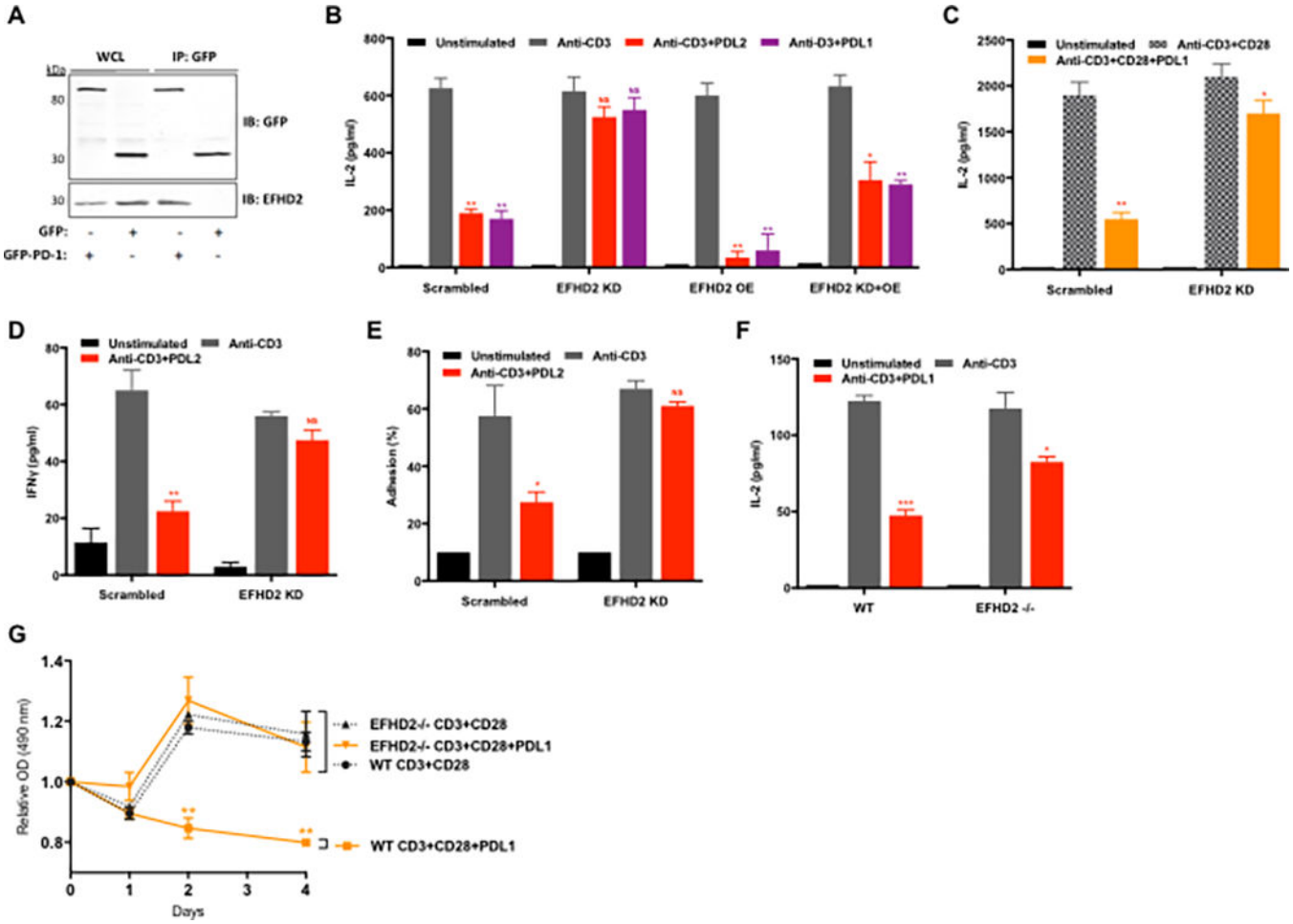

Figure 2. EFHD2 is required for PD-1 inhibitory functions.

(**A**) Jurkat T cells were transiently transfected with GFP-PD-1 or GFP alone, whole-cell lysates (WCL) were incubated with anti-GFP antibody and immunoprecipitated proteins were detected by immunoblotting, as indicated. A eepresentative blot of three independent experiments is shown. (**B-D**) Freshly isolated human CD3 T cells were transfected with non-targeting control siRNA (Scrambled) or with siRNA targeting *EFHD2* or with EFHD2 expression plasmids, as indicated. 24 hours later, cells were stimulated with magnetic beads coated with anti-CD3 or anti-CD3+PDL2 or anti-CD3+PDL1 or anti-CD3+CD28 or anti-CD3+CD28+PDL1, as indicated. After additional 24 hours media was harvested, and IL-2 or IFN-γ levels were measured by ELISA. EFHD2 OE stands for EFHD2 Over Expression, which was rescued by expressing EFHD2 lacking the 3-UTR. (**E**) Jurkat T cells, stably transfected with shRNA targeting *EFHD2* or a control non-targeting shRNA (Scrambled) were stimulated as indicated and subjected to static adhesion assay to fibronectin-coated wells. (**F**) Freshly isolated mouse T cells from wild type (WT) mice or *EFHD2* knockout ($EFHD2^{-/-}$) mice were stimulated with magnetic beads coated with anti-CD3 or anti-CD3+PDL2 for 48 hours. IL-2 levels in the media were measured by ELISA. (**G**) Freshly isolated mouse T cells from WT mice or EFHD2 knockout mice were stimulated with magnetic beads, as indicated, and cell proliferation was monitored using the MTS assay. Values are expressed as increase in OD compared with day 0. All the experiments were done

at least three times (n≥3), * $p<0.05$, ** $p<0.001$, *** $p<0.0001$, NS (not significant), unpaired student *t*-test.

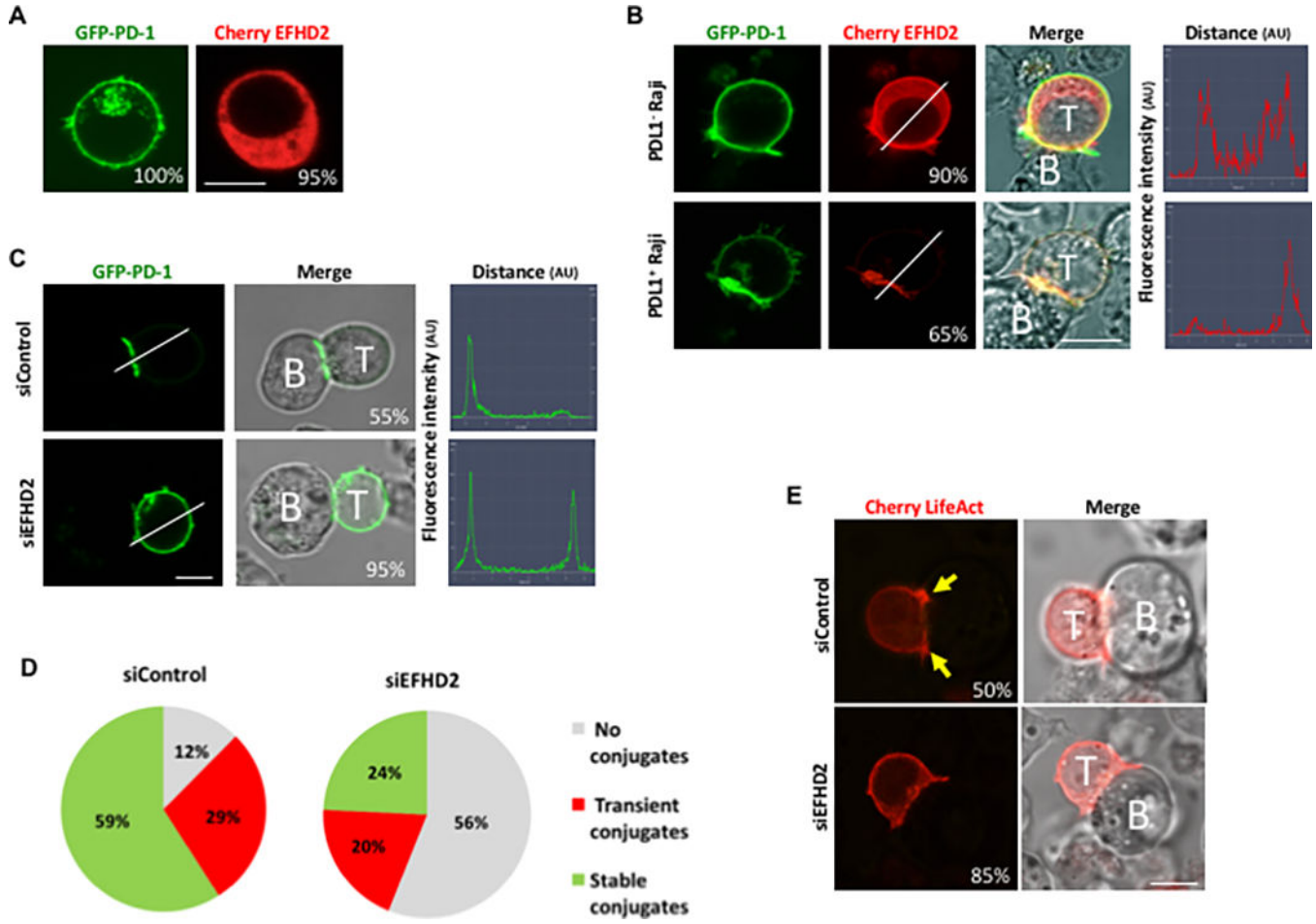

Figure 3. EFHD2 co-localizes with PD-1 in the immunological synapse.

(**A**) Jurkat T cells were transfected with the indicated expression plasmids and imaged by confocal microscopy. Images are representative of at least 50 cells from each of three independent experiments. The percentage of the dominant phenotype for each condition is shown. Bars are 10 μm. (**B**) Jurkat T cells were transfected with the indicated expression vectors prior to co-culturing with Raji B cells that either express or not the ligand PDL1 and loaded with SEE. Images are representative of at least 50 cells from each of three independent experiments. The percentage of the dominant phenotype for each condition is shown. Bars are 10 μm. Line analysis shows fluorescent intensities of EFHD2 along the diameter of the cell. (**C**) Freshly isolated human T cells were transfected with non-targeting siRNA (siControl) or siRNA targeting EFHD2 (siEFHD2) and with GFP-PD-1 expression plasmid, followed by co-culturing with Raji B cells expressing PDL1 and loaded with SEE. Cells were subjected to real-time imaging by confocal microscopy. Images are representative of at least 50 cells from each of three independent experiments. The percentage of the dominant phenotype for each condition is shown. Bars 10 μm. Line analysis shows fluorescent intensities of GFP-PD-1 along the diameter of the cell. (**D**) Percentage of transient and stable conjugates. Mean of five independent experiments is shown. (**E**) Freshly isolated human T cells were transfected with Cherry LifeAct and with non-targeting siRNA (siControl) or siRNA targeting EFHD2 (siEFHD2), followed by co-culturing with Raji B

cells expressing PDL1 and loaded with SEE. Images are representative of at least 50 cells from each of four independent experiments. Arrows indicate actin accumulation. The percentage of the dominant phenotype for each condition is shown. Bars 10 μm.

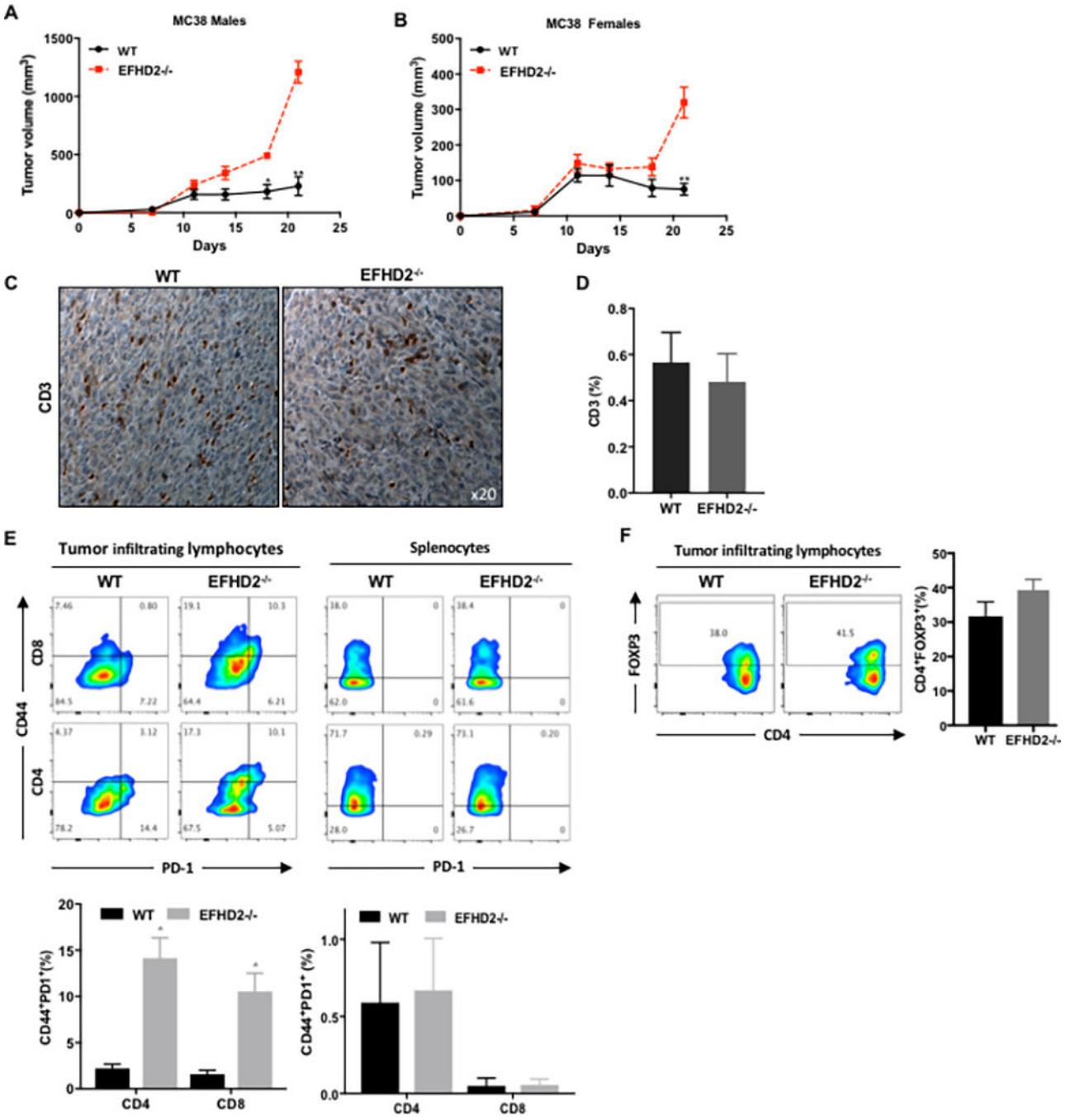

Figure 4. EFHD2 is necessary for anti-tumor immune response in vivo.

MC38 cells were inoculated into EFHD2 deficient male mice (**A)** or female mice (**B**) and into wild type (WT) littermates. After tumor inoculation (day 0), tumor volume was measured as described in the method section. Results are expressed as mean ± SEM; n=4 per group. (**C**) Immune histochemical staining in two representative tumor sections. Magnification ×20. (**D-F**) Single-cell suspensions from tumor tissues and spleens were analyzed by fluorescence-activated cell sorter. Results are shown as percentage of indicated subset in particular immune cell population. (**D**) Percentage of CD45/CD3 positive cells of

total tumor cells. (**E**) Expression of CD44 and PD-1 on splenocytes and tumor-infiltrating CD8 and CD4 cells from MC38 tumor-bearing mice. Bar graphs representing percentages of the CD44/PD-1 expressing populations is shown at the bottom. (**F**) Flow cytometric analysis depicting percentages of FOXP3 positive cells on tumor-infiltrating CD4 T cells from MC38 tumor-bearing mice. Bar graphs representing percentages of the CD4/FOXP3 expressing population is shown on the right. All the experiments were done at least three times (n≥3), * $p<0.05$, ** $p<0.001$.

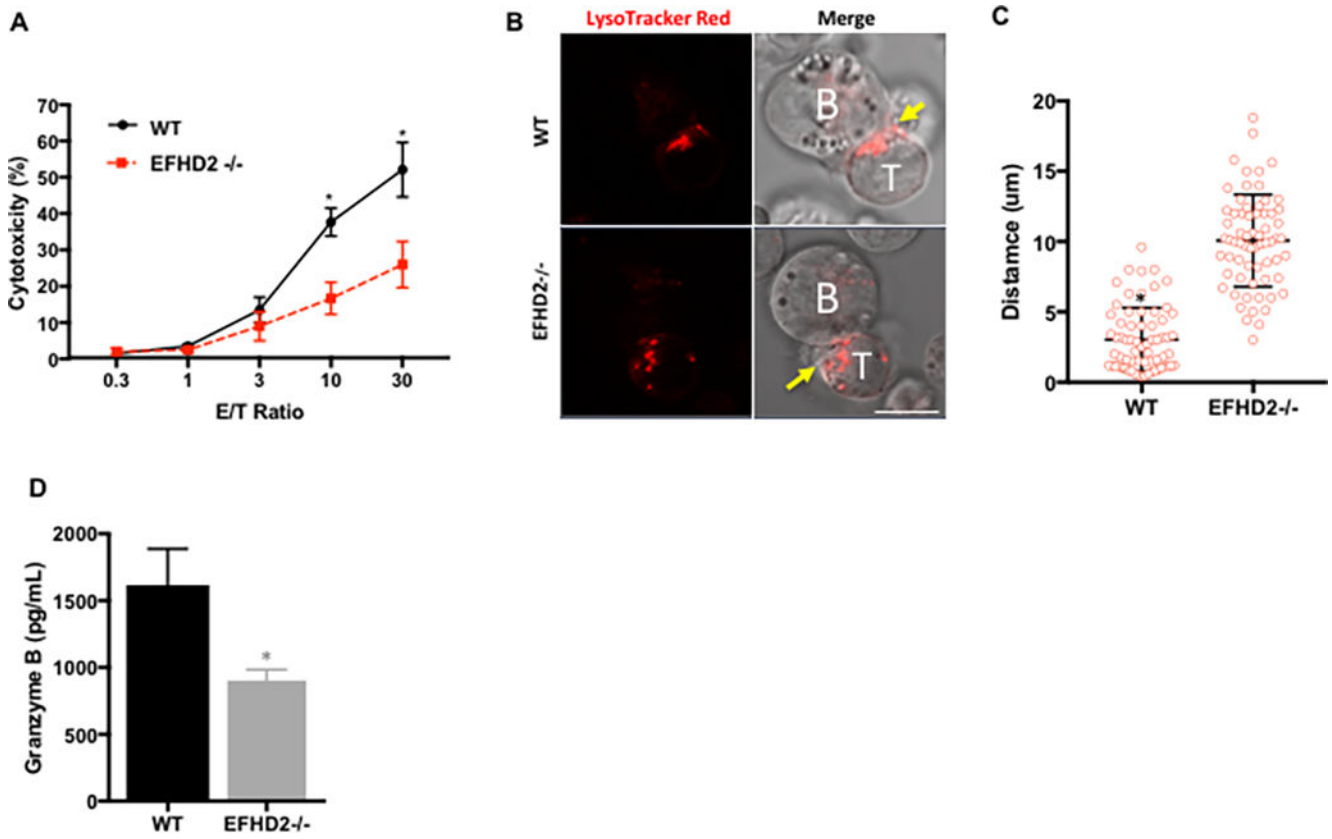

Figure 5. EFHD2 is required for T cell induced cytotoxicity.

(**A**) WT control and EFHD2$^{-/-}$ CD8 T cells were used as effector cells toward SEE-loaded Raji target cells in 4 hours cytotoxicity LDH release assay. (**B**) A representative images of the localization of lytic granules in CD8 T cells from WT and EFHD2$^{-/-}$ mice following co-culturing with Raji target cells. Arrows indicated granule localization. Bars 10 μm. (**C**) Distance of granules from the contact area between the cells within 5 minutes of synapse formation. 50–70 individual granules were counted from multiple cells acquired through three independent experiments. Data represent the mean ± SEM. * p<0.05. (**D**) CD8 T cell from either WT or EFHD2$^{-/-}$ were co-cultured with SEE loaded Raji target cells and levels of released Granzyme B was measure by ELISA. (n=3), * p<0.05.

Table 1.

Immune, cytoskeleton and synapse related interactions of the PD-1 tail.

Gene	UniProt ID	Peptide spectrum match
PFN1	P07737	20
PTPN11	Q06124	17
GRB2	P62993	15
MYO5A	Q9Y4I1	13
TLN1	Q9Y490	11
EFHD2	Q96C19	7
PDIA3	P30101	7
VAV1	P15498	5
ATP2A2	P16615	5
ANXA1	P04083	5
RPL22	P3528	5
EVL	Q9UI08	4
CAPN1	P07384	4
DOCK2	Q92608	4
PSMC4	P43686	3
ELMO1	Q92556	2
ITK	Q08881	2
RAF1	P04049	2
DYNLL1	P63167	2